




Radiofrequency ablation using a novel insulated-tip ablation catheter can create uniform lesions comparable in size to conventional irrigated ablation catheters while using a fraction of the energy and irrigation

Arash Aryana MD, PhD¹  | Ramiro M. Irastorza PhD^{2,3} | Enrique Berjano PhD⁴  | Richard J. Cohen MD, PhD⁵ | Jeffrey Kraus BS⁶ | Ali Haghghi-Mood PhD⁶ | Vivek Y. Reddy MD⁷  | André d'Avila MD, PhD⁸

¹Mercy General Hospital and Dignity Health Heart and Vascular Institute, Sacramento, California, USA

²Instituto de Física de Líquidos y Sistemas Biológicos (CONICET), La Plata, Argentina

³Instituto de Ingeniería y Agronomía, Universidad Nacional Arturo Jauretche, Florencio Varela, Argentina

⁴BioMIT, Department of Electronic Engineering, Universitat Politècnica de València, Valencia, Spain

⁵Institute for Medical Engineering and Science, Massachusetts Institute of Technology, Cambridge, Massachusetts, USA

⁶Sirona Medical Technologies, Inc, Windsor, Connecticut, USA

⁷Helmsley Cardiac Arrhythmia Service, Mount Sinai School of Medicine, New York, New York, USA

⁸Beth Israel Deaconess Medical Center, Boston, Massachusetts, USA

Correspondence

Arash Aryana, MD, PhD, Mercy General Hospital and Dignity Health Heart and Vascular Institute, 3941 J St, Suite #350, Sacramento, CA 95819, USA.

Email: a_aryana@outlook.com

Funding information

Sirona Medical Technologies, Inc; The Proyecto UNAJ Investiga 2017, Grant/Award Number: 80020170100019UJ; The Spanish Ministerio de Ciencia, Innovación y Universidades/ Agencia Estatal de Investigación (MCIN/AEI/ 10.13039/501100011033), Grant/Award Number: RTI2018-094357-B-C21

Abstract

Introduction: During radiofrequency ablation (RFA) using conventional RFA catheters (RFC), ~90% of the energy dissipates into the bloodstream/surrounding tissue. We hypothesized that a novel insulated-tip ablation catheter (SMT) capable of blocking the radiofrequency path may focus most of the energy into the targeted tissue while utilizing reduced power and irrigation.

Methods: This study evaluated the outcomes of RFA using SMT versus an RFC in silico, ex vivo, and in vivo. Radiofrequency applications were delivered over porcine myocardium (ex vivo) and porcine thigh muscle preparations superfused with heparinized blood (in vivo). Altogether, 274 radiofrequency applications were delivered using SMT (4–15 W, 2 or 20 ml/min) and 74 applications using RFC (30 W, 30 ml/min).

Results: RFA using SMT proved capable of directing 66.8% of the radiofrequency energy into the targeted tissue. Accordingly, low power–low irrigation RFA using SMT (8–12 W, 2 ml/min) yielded lesion sizes comparable with RFC, whereas high

Disclosure Drs. Aryana, Cohen, and Reddy have received consulting fees from Sirona Medical Technologies, Inc. Dr. Haghghi-Mood and Mr. Kraus are employees of Sirona Medical Technologies, Inc. Drs. Aryana, Cohen, Reddy, Haghghi-Mood, and Mr. Kraus hold equity in Sirona Medical Technologies, Inc. Other authors: No disclosures.

This is an open access article under the terms of the Creative Commons Attribution-NonCommercial License, which permits use, distribution and reproduction in any medium, provided the original work is properly cited and is not used for commercial purposes.

© 2022 The Authors. *Journal of Cardiovascular Electrophysiology* published by Wiley Periodicals LLC.

power–high irrigation (15 W, 20 ml/min) RFA with SMT yielded lesions larger than RFC ($p < .05$). Although SMT was associated with greater impedance drops *ex vivo* and *in vivo*, ablation using RFC was associated with increased charring/steam pop/tissue cavitation ($p < .05$). Lastly, lesions created with SMT were more homogeneous than RFC ($p < .001$).

Conclusion: Low power–low irrigation (8–12 W, 2 ml/min) RFA using the novel SMT ablation catheter can create more uniform, but comparable-sized lesions as RFC with reduced charring/steam pop/tissue cavitation. High power–high irrigation (15 W, 20 ml/min) RFA with SMT yields lesions larger than RFC.

KEYWORDS

catheter ablation, power, radiofrequency, SMT, steam pop

1 | INTRODUCTION

Radiofrequency (RF) is the most widely used energy modality for catheter ablation of cardiac arrhythmias.¹ RF ablation (RFA) results in myocardial cell destruction through thermal energy, namely, resistive and conductive heating.² Tissue temperatures $>50^{\circ}\text{C}$ are required for irreversible myocardial injury, whereas temperatures $>100^{\circ}\text{C}$ can result in coagulum formation on the electrode tip and loss of effective heating.² Meanwhile, ablation using the currently approved, conventional RFA catheters (RFC) is strikingly inefficient as $\sim 90\%$ of the applied energy dissipates into the bloodstream or the surrounding/nontargeted tissue.³ Thus, we hypothesized that a novel ablation catheter with an insulated tip (SMT, Sirona Medical Technologies), capable of blocking the path of RF energy, may divert a significantly greater magnitude of the delivered energy into the targeted tissue while requiring reduced power and irrigation, but still creating lesions comparable in size to those generated with a standard, irrigated 3.5-mm tip RFA catheter.

2 | METHODS

We created a computational (*in silico*) model to evaluate the performances of SMT versus an RFC (ThermoCool, Biosense Webster, Inc.). In addition, we delivered and analyzed a total of 348 RF applications *ex vivo* ($n = 267$) and *in vivo* ($n = 81$), using SMT ($n = 274$) and RFC ($n = 74$). The experimental protocol was approved by the Institutional Animal Care and Use Committee at the Sutter Institute for Medical Research (Sacramento, CA) and performed according to institutional guidelines.

2.1 | SMT ablation catheter

The SMT ablation catheter is a 9-French, open-irrigated ablation catheter (irrigation rate: 2 ml/min) with a novel design that consists of

a central electrode (2.3×4 mm), surrounded by four peripheral electrodes (1×2 mm, each) for both RF and pulsed field ablation. The design is intended to insulate the central electrode, which is surrounded by an insulating dielectric as well as a flexible metallic braid that acts as a Faraday cage. This structure was specifically devised to minimize the passage of RF energy into the bloodstream and the surrounding tissue, thereby directing the majority of the energy into the targeted tissue. The ablation catheter can be deployed and used in “vector” or “linear” configurations (Figure 1). In the vector conformation, the four flexible deployable wings serve as a “landing gear,” intended to provide stable tissue contact and maintain a consistent electrode–tissue interface. The flexible wing structure is designed with the intent to improve catheter stability in both configurations while reducing the likelihood of tissue injury/perforation.

Additionally, the SMT catheter can also be used for multi-electrode activation mapping of focal arrhythmias. When used for this purpose, the peripheral electrode array is expanded into the vector configuration, such that the central and the four peripheral electrodes are placed in contact with the tissue. As input data, the mapping system utilizes the XY locations of the five electrodes on the array as captured on a stationary fluoroscopic image as well as the arrival times of a wavefront emanating from the arrhythmia's site of origin. The system software then utilizes the input data to triangulate the location of the arrhythmia's site of origin. Once the site has been specifically localized in three-dimensional space, it is projected onto a fluoroscopy image to allow the operator to advance the catheter to the site of arrhythmia origin for energy delivery and ablation.

2.2 | In silico study

We generated a computational model to elucidate the magnitude of RF energy directed into the targeted tissue using both SMT and RFC. The model included a perpendicular catheter orientation placed on a fragment of cardiac tissue surrounded by circulating blood. The

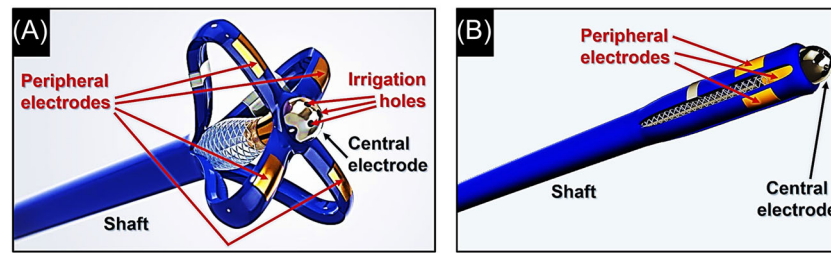


FIGURE 1 The design of the SMT ablation catheter. SMT is a 9-French, open-irrigated ablation catheter, which consists of a central electrode measuring 2.3 mm × 4 mm, surrounded by four peripheral electrodes. The insulated-tip design is intended to block the path of RF into the bloodstream and the surrounding tissue, to focus a greater magnitude of the delivered energy into the targeted tissue. The ablation catheter can be deployed and used in “vector” (A) or “linear” (B) configurations. In the vector configuration, the four deployable wings serve as a “landing gear,” intended to provide greater catheter stability and tissue contact during mapping and ablation.

COMSOL Multiphysics program (COMSOL) was used to create the finite element model for conducting computer simulations. The irrigation was modeled by fixing the temperature at the corresponding zone with the average value derived from *ex vivo* experiments. RFA was simulated for SMT at 6, 8, 10, and 12 W and for RFC at 30 W, both for a duration of 30 s. The electrical characteristics of the tissue were adjusted to match the baseline impedance values. Lesion sizes were computed using isolines ($\Omega = 1$) from the Arrhenius thermal injury model.

2.3 | Ex vivo study

Sections of normal, nonperfused porcine ventricular myocardium were suspended in a fixture inside a tissue bath containing a solution of circulating saline (temperature: $37.1 \pm 1.3^\circ\text{C}$). Altogether, 267 RF applications were delivered, including 167 applications using SMT at low power–low irrigation (2 ml/min) for 15 s ($n = 25$), 30 s ($n = 75$), 60 s ($n = 44$), and 90 s ($n = 23$) at 4, 5, 6, 7, 8, 9, 10, 11, and 12 W and 40 applications using high power–high irrigation (15 W, 20 ml/min) for 30 s ($n = 20$) and 60 s ($n = 20$), versus 60 applications using RFC at 30 W and 30 ml/min for 15 s ($n = 10$), 30 s ($n = 20$), 60 s ($n = 20$), and 90 s ($n = 10$).

2.4 | In vivo study

We employed the previously described swine thigh muscle preparation model to compare lesions created using the RFC versus SMT catheters.⁴ Two healthy swine weighing 50–55 kg were anesthetized with a continuous infusion of fentanyl (157 mcg), ketamine (1000 mg), and midazolam (30 mg) and mechanically ventilated. The right carotid artery was cannulated for monitoring arterial pressure. Each swine was initially placed on its left side. A 20-cm skin incision was made over the right thigh muscle. An adhesive electro-surgical dispersive pad (20 × 10 cm) was applied to the shaved flank. The skin on each side of the incision was dissected free of the connective tissue. The skin edges were raised to form a cradle that was superfused with heparinized blood (activated clotting time > 300 s) at

37°C . After each RF application, the catheter was left in place and the circulating blood was removed from the cradle. The ablation electrode and the electrode–tissue interface were examined for thrombus. The electrode was then removed, cleaned, and positioned at a new site for the subsequent application. RF lesions were applied at multiple sites along the surface of the right thigh muscle, preserving adequate distance in-between to avoid overlap. The skin incision was then closed and the animal was rotated to expose the left thigh muscle. The left thigh was then prepared in a similar method with RF applications delivered in the same manner to multiple sites along the surface of the left thigh muscle.

Altogether, 81 RF applications were delivered, including 67 RF applications using low power–low irrigation (2 ml/min) with SMT for 30 s ($n = 41$) and 60 s ($n = 26$) at 6, 8, 10, or 12 W versus 14 applications with RFC at 30 W and 30 ml/min for 30 s ($n = 5$) or 60 s ($n = 9$). Upon completion of the study, the animals were euthanized and the ablated thigh muscle tissue surgically harvested for gross pathology.

2.5 | Lesion analysis

RFA was always performed with ablation catheters positioned in a perpendicular orientation. A CoolFlow pump (Biosense Webster) and a Stockert RFA generator (Biosense Webster) were used with both RFA catheters. All ablation parameters including impedance, temperature, and power were recorded along with incidences of steam pop, charring, and tissue cavitation. All lesion dimensions were determined using a digital micrometer. Lesion volume was determined using the following formula⁵:

$$\text{Lesion volume} = \left[1.33 \times \pi \times \text{depth} \left(\frac{\text{maximum diameter}}{2} \right) \times \left(\frac{\text{surface diameter}}{2} \right) \right] / 2.$$

In addition, a quantitative analysis was performed to characterize the homogeneity of lesions created *ex vivo*. The image of each lesion

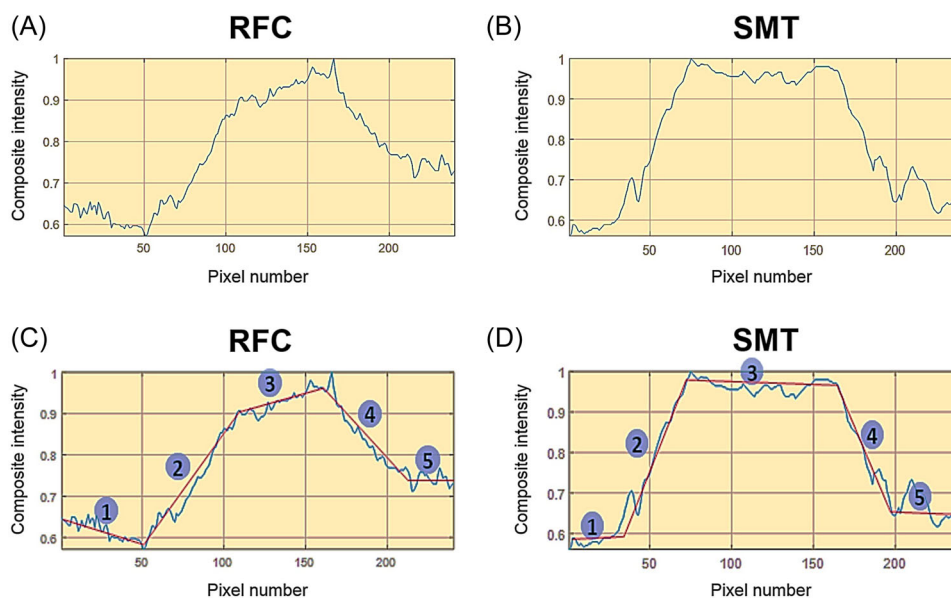


FIGURE 2 Assessment of lesion homogeneity using RFC and SMT. RF lesion homogeneity was assessed by analyzing RGB images of ablation lesions and creating composite intensity graphs for RFC (A) and SMT (B) which were then represented by five best-fit connected line segments. Subsequently, the width of the central maximally ablated segment was compared with the widths of the adjacent partially ablated segments to obtain a homogeneity score for RFC (C) and SMT (D). RGB, red–green–blue; RF, radiofrequency; RFC, radiofrequency ablation catheters

was decomposed into red–green–blue (RGB) components. For each lesion, composite intensity graphs were generated for variation of the composite intensity $[(R + G + B)/3]$ across the X and Y axes and represented by five best-fit connected line segments (Figure 2). Subsequently, the ratio of (i) the width of the central segment (region of maximum ablation) to (ii) the sum of the widths of the central segment and the two adjacent segments (regions of partial ablation) was calculated along the X and Y axes. The two ratios were then averaged to yield an ablation homogeneity score for each lesion.

2.6 | Statistical methods

The data are represented as mean \pm standard deviation. Continuous variables were analyzed using a two-sample *t* test. All *p* values were two-sided and a *p* value of <0.05 was considered statistically significant. The analyses were conducted using Stata 14 (StataCorp LP).

3 | RESULTS

3.1 | Computational model findings

The computer model predicted the tendency observed in experiments in terms of lesion size and impedance drop. Specifically, SMT created lesions with comparable dimensions to RFC with surface diameters ranging between 5.6 and 6.5 mm (SMT at 6–12 W) versus

6.4 mm with RFC (30 W) and lesion depths measuring 4.3–5.6 mm (SMT at 6–12 W) versus 5.1 mm with RFC (30 W). The magnitude of impedance drop during RFA was significantly greater with SMT as compared to RFC (24%–26% vs. 10%), with a roll-off (a sudden impedance increase) beyond 12 W.

Assuming a patient impedance of $40 \Omega^3$, the computer model found that with RFC only 13.7% of the RF energy was delivered in the targeted tissue, 58.3% of the energy was removed by bloodstream, and 28% dissipated in the remote patient tissues. In contrast, with SMT 66.8% of the energy was directed into the targeted tissue, 13.2% was removed by bloodstream, and 20% was lost in the remote tissues (Figure 3). The model further demonstrated that due to the greater electrical conductivity of blood versus myocardium, even in a hypothetical (“ideal”) scenario in which the ablation electrode is not in direct contact with the blood pool, a portion of RF energy after entering the tissue, still passes through the tissue, back into the bloodstream.

3.2 | Ex vivo findings

Ex vivo, 49 applications using SMT were delivered in a linear configuration, whereas 118 applications were applied in a vector mode. Table 1 depicts the RFA data for each of the two catheters. There was a dose-dependent response observed in lesion size with SMT as a function of power (Figure 4). SMT lesion sizes did not differ significantly in vector versus linear modes ($p > .05$). Lesions created with low power–low irrigation RFA using SMT at 8–12 (2 ml/min)

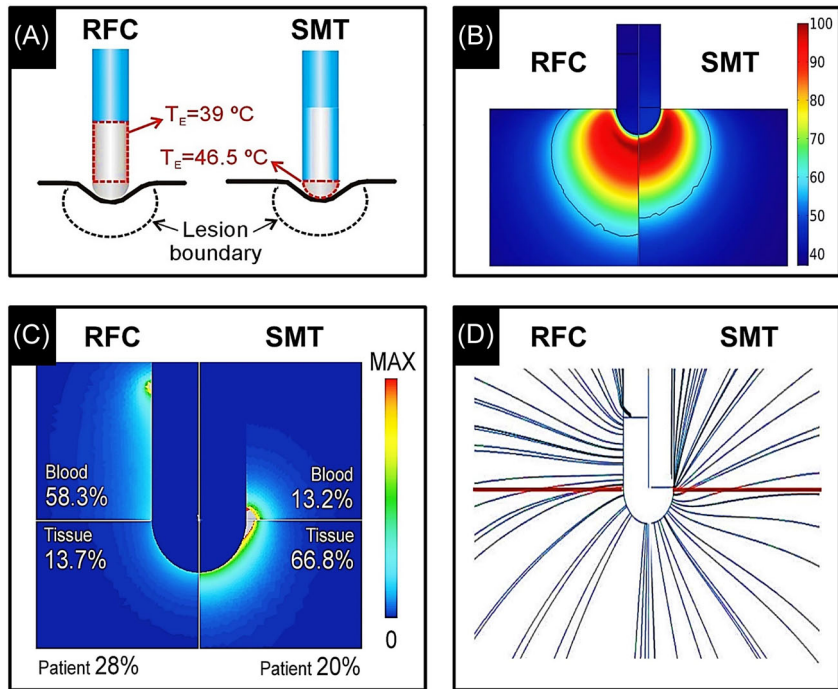
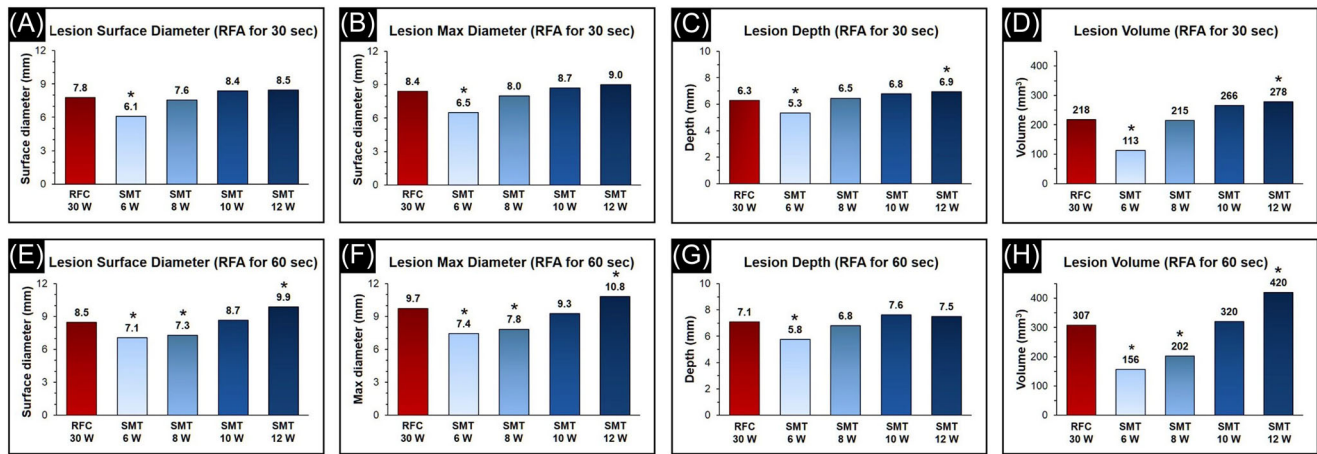


FIGURE 3 Computational modeling of RFC versus SMT. (A) Irrigation in SMT and RFC (ThermoCool) was modeled by fixing the electrode temperature (T_E) in a specific zone of the electrode. (B) Temperature distributions (scale in °C) and lesion boundaries for each catheter. (C) Spatial distributions of RF energy density (W/m^3) applied around the electrode for each catheter. The values represent percentages of total RF energy dissipating into the blood, the targeted tissue, and the patient. As seen, a significantly greater proportion of the RF energy is directed into the targeted tissue with SMT (66.8%) versus RFC (13.7%). (D) Electrical current lines computed for each catheter. RF, radiofrequency; RFC, radiofrequency ablation catheters

TABLE 1 RFA and lesion characteristics using low power–low irrigation RFA with SMT at 8, 10, and 12 W (2 ml/min) versus RFC at 30 W (30 ml/min) for 30 and 60 s ex vivo and in vivo

Ablation parameters	SMT (n = 115)						RFC (n = 54)	
	8	10	10	12	12	30	30	
Power, W	8	10	10	12	12	30	30	
Irrigation flow rate, ml/min	2	2	2	2	2	30	30	
Application duration, s	30	60	30	60	30	60	60	
Ex vivo								
Maximum ablation temperature, °C	44 ± 6	44 ± 5	47 ± 5	46 ± 5	47 ± 4	44 ± 2	36 ± 4	36 ± 3
Baseline impedance, Ω	194 ± 19	183 ± 11	201 ± 21	189 ± 13	187 ± 61	195 ± 10	98 ± 5	97 ± 6
Drop in impedance, %	28 ± 5	28 ± 3	29 ± 9	34 ± 5	30 ± 8	38 ± 3	22 ± 3	22 ± 4
Lesion size								
Surface diameter, mm	7.6 ± 1.4	7.3 ± 0.8	8.4 ± 1.1	8.7 ± 0.7	8.5 ± 0.9	9.9 ± 0.5	7.8 ± 1.1	8.0 ± 1.2
Maximum diameter, mm	8.0 ± 1.4	7.8 ± 0.4	8.7 ± 1.3	9.3 ± 0.9	9.0 ± 0.7	10.8 ± 0.8	8.4 ± 0.9	9.7 ± 0.7
Depth, mm	6.5 ± 1.0	6.8 ± 0.6	6.8 ± 0.9	7.6 ± 0.4	6.9 ± 0.5	7.5 ± 0.5	6.3 ± 0.7	7.1 ± 0.8
Volume, mm ³	215 ± 27	202 ± 24	266 ± 91	320 ± 53	278 ± 62	420 ± 51	218 ± 56	307 ± 72
In vivo								
Maximum ablation temperature, °C	40 ± 7	46 ± 6	41 ± 5	50 ± 11	45 ± 8	47 ± 11	38 ± 1	40 ± 4
Baseline impedance, Ω	216 ± 50	215 ± 56	235 ± 54	228 ± 53	229 ± 56	233 ± 52	133 ± 14	127 ± 10
Drop in impedance, %	25 ± 6	32 ± 8	31 ± 7	34 ± 8	35 ± 11	35 ± 10	17 ± 3	18 ± 7
Lesion size								
Surface diameter, mm	6.1 ± 1.1	7.3 ± 1.2	6.5 ± 1.3	8.2 ± 1.0	7.3 ± 0.9	8.4 ± 0.4	6.6 ± 1.0	8.1 ± 1.4
Maximum diameter, mm	6.7 ± 1.6	8.3 ± 1.7	7.1 ± 1.2	9.4 ± 1.7	7.8 ± 0.9	9.9 ± 1.5	8.2 ± 1.9	9.4 ± 1.4
Depth, mm	4.3 ± 0.8	5.8 ± 0.8	4.5 ± 0.5	6.2 ± 1.1	5.1 ± 0.5	6.0 ± 1.1	5.0 ± 0.9	4.9 ± 1.2
Volume, mm ³	97 ± 53	193 ± 83	111 ± 37	248 ± 60	154 ± 48	267 ± 87	149 ± 71	200 ± 96

Abbreviations: RFA, radiofrequency ablation; RFC, radiofrequency ablation catheter.



* Significant P-value

FIGURE 4 RF lesion sizes created using RFC and SMT ex vivo. Lesion dimensions including surface diameter, maximum (max) diameter, depth, and volume using RFC (ThermoCool) at 30 W and SMT using varying power (6, 8, 10, and 12 W) for 30 s (A–D) and 60 s (E–H), respectively. RF, radiofrequency; RFC, radiofrequency ablation catheter

TABLE 2 Ex vivo RFA and lesion characteristics using SMT at high power–high irrigation (15 W, 20 ml/min) versus RFC (30 W, 30 ml/min) for 30 and 60 s

Ablation parameters	30 s (n = 40)		p value	60 s (n = 40)		p value
	SMT	RFC		SMT	RFC	
Ablation catheter	SMT	RFC	–	SMT	RFC	–
Power, W	15 ± 0	30 ± 0	<.001*	15 ± 0	30 ± 0	<.001*
Irrigation flow rate, ml/min	20 ± 0	30 ± 0	<.001*	20 ± 0	30 ± 0	<.001*
Maximum ablation temperature, °C	34 ± 3	36 ± 3	.06	36 ± 4	36 ± 3	.73
Baseline impedance, Ω	157 ± 10	98 ± 5	<.001*	171 ± 14	97 ± 6	<.001*
Drop in impedance, %	34 ± 4	22 ± 3	<.001*	34 ± 5	22 ± 4	<.001*
Lesion size						
Surface diameter, mm	8.4 ± 0.4	7.8 ± 1.1	.001*	9.1 ± 0.8	8.5 ± 0.9	.04*
Maximum diameter, mm	9.2 ± 0.5	8.0 ± 0.9	<.001*	10.8 ± 0.6	9.7 ± 1.2	.001*
Depth, mm	8.9 ± 0.8	6.3 ± 0.7	<.001*	9.4 ± 1.0	7.1 ± 0.8	<.001*
Volume, mm ³	358 ± 49	218 ± 56	<.001*	481 ± 94	307 ± 74	<.001*

Abbreviations: RFA, radiofrequency ablation; RFC, radiofrequency ablation catheter.

*Significant p value.

were comparable to those generated with RFC at 30 W (30 ml/min) for both 30 and 60 s (mean duration: 45 ± 15 s), including surface diameter (8.4 ± 1.3 mm vs. 8.1 ± 1.0 mm, $p = .32$), maximum diameter (8.9 ± 1.4 mm vs. 9.1 ± 1.2 mm, $p = .51$), depth (7.0 ± 0.8 mm vs. 6.7 ± 0.8 mm, $p = .06$) and volume (282 ± 100 mm³ vs. 263 ± 79 mm³, $p = .28$), respectively. However, the mean impedance drop during RFA was significantly greater with SMT (31 ± 7%) versus RFC (22 ± 4%), $p < .001$. Furthermore, lesions were significantly smaller at 15 versus 90 s of RFA using SMT, including surface diameter (6.6 ± 0.8 mm vs. 9.2 ± 0.9 mm, $p < .001$), maximum diameter (7.3 ± 0.6 mm vs. 11.0 ± 1.7 mm, $p < .001$), depth (5.4 ± 0.9 mm vs. 7.5 ± 0.5 mm, $p < .001$) and volume (137 ± 40 mm³ vs. 314 ± 90 mm³, $p < .001$). Similarly, lesions were generally smaller when comparing 30 versus 60 s (surface diameter

[$p = .12$], maximum diameter [$p = .03$], depth [$p = .003$], and volume [$p = .02$]) and when comparing 30 versus 90 s (surface diameter [$p = .003$], maximum diameter [$p < .001$], depth [$p = .002$], and volume [$p < .001$]). Altogether, there were 8 (12.9%) steam pops with SMT at 8–12 W (2 ml/min) versus 12 (30.0%) with RFC at 30 W (30 ml/min), $p = .03$. No charring or tissue cavitation were observed with either catheter. RFA parameters for applications resulting in a steam pop are presented in Table 3.

On the other hand, high power–high irrigation (15 W, 20 ml/min) RFA using SMT generated lesions much larger than RFC (Table 2). Two steam pops (5.0%) occurred with SMT during high power–high irrigation RFA versus 12 (30.0%) with RFC ($p = .003$). No charring or tissue cavitation was encountered during high power–high irrigation RFA with SMT.

Furthermore, lesions created with SMT were more homogenous and exhibited sharper (narrower) zones of transition as compared to RFC (Figure 5). This was evident by the ablation homogeneity scores which measured $69 \pm 3\%$ for SMT versus $43 \pm 2\%$ for RFC, respectively ($p < .001$).

3.3 | In vivo findings

All in vivo SMT applications were performed in a vector mode. Once again, there were no significant differences in lesion dimensions when comparing low power-low irrigation RFA with SMT at 8–12 W (2 ml/min) versus RFC at 30 W (30 ml/min) for a duration of 30 s (Table 1). The measurements were as follows: surface diameter: 6.6 ± 1.2 mm (SMT) versus 6.6 ± 1.0 mm (RFC), $p = .91$, maximum diameter: 7.2 ± 1.3 mm (SMT) versus 8.2 ± 2.0 mm (RFC), $p = .13$, depth: 4.6 ± 0.7 mm (SMT) versus 5.0 ± 1.0 mm (RFC), $p = .27$, and volume: 120 ± 49 mm³ (SMT) versus 148 ± 64 mm³ (RFC), $p = .27$. Likewise, there were no differences in lesion sizes for 60 s applications; surface diameter: 8.0 ± 1.0 mm (SMT) versus 8.1 ± 1.4 mm (RFC), $p = .71$, maximum diameter: 9.3 ± 1.7 mm (SMT) versus 9.4 ± 1.4 mm (RFC),

$p = .86$, depth: 6.0 ± 1 mm (SMT) versus 4.9 ± 1.2 mm (RFC), $p = .01$, and volume: 238 ± 79 mm³ (SMT) versus 200 ± 96 mm³ (RFC), $p = .28$. However, low power-low irrigation RFA using SMT at 6 W yielded lesions that were typically smaller than those created with RFC at 30 W (Figure 6). The measurements were as follows for 30 s applications; surface diameter: 5.3 ± 1.7 mm (SMT) versus 6.6 ± 1.0 mm (RFC), $p = .17$, maximum diameter: 5.7 ± 1.9 mm (SMT) versus 8.2 ± 2.0 mm (RFC), $p = .04$, depth: 3.9 ± 0.7 mm (SMT) versus 5.0 ± 1.0 mm (RFC), $p = .04$, and volume: 73 ± 56 mm³ (SMT) versus 148 ± 71 mm³ (RFC), $p = .06$. The same was observed for 60 s applications; surface diameter: 5.9 ± 1.4 mm (SMT) versus 8.1 ± 1.4 mm (RFC), $p = .01$, maximum diameter: 6.6 ± 2.2 mm (SMT) versus 9.4 ± 1.4 mm (RFC), $p = .01$, depth: 4.5 ± 0.8 mm (SMT) versus 4.9 ± 1.2 mm (RFC), $p = .50$, and volume: 103 ± 82 mm³ (SMT) versus 200 ± 96 mm³ (RFC), $p = .07$.

As observed in silico and ex vivo, the impedance drop during RFA was overall greater with SMT versus RFC ($31 \pm 10\%$ vs. $18 \pm 6\%$; $p < .001$). Two (14.3%) steam pops were observed with RFC versus none (0%) with SMT, $p = .001$. Furthermore, one case of charring (7.1%) and one tissue cavitation (7.1%) also occurred with RFC, but none (0%) with SMT, $p = .03$ (Figure 7). RFA parameters for applications resulting in a steam pop are depicted in Table 3.

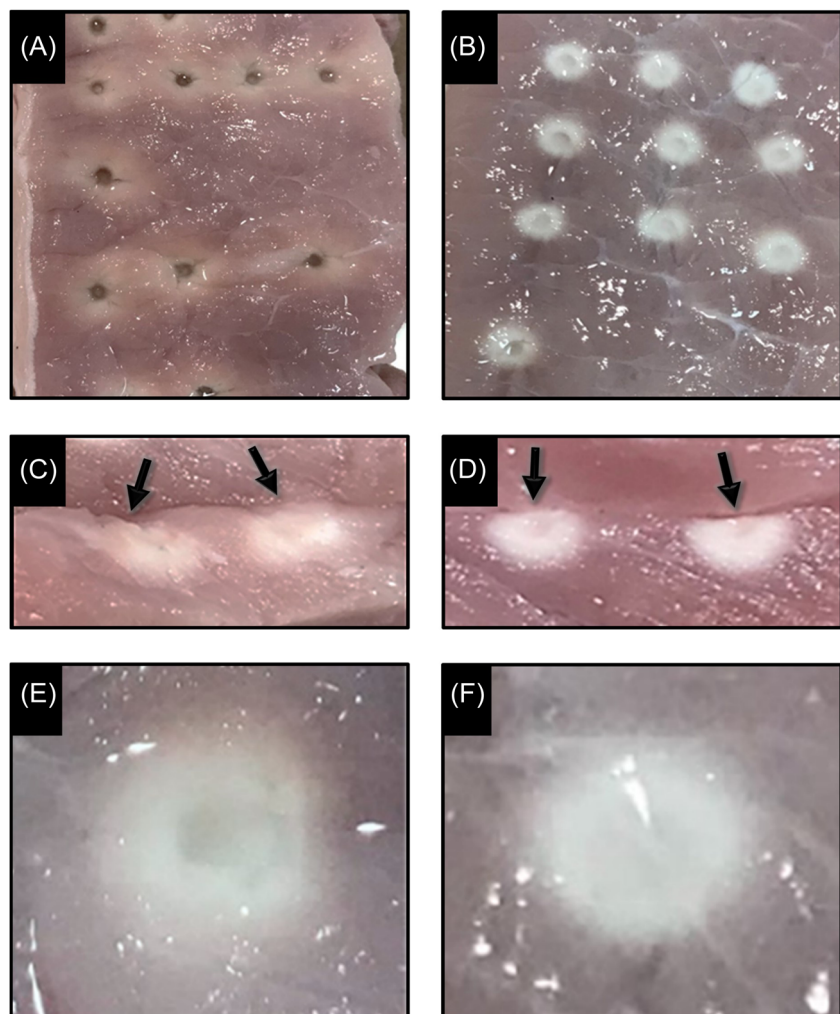
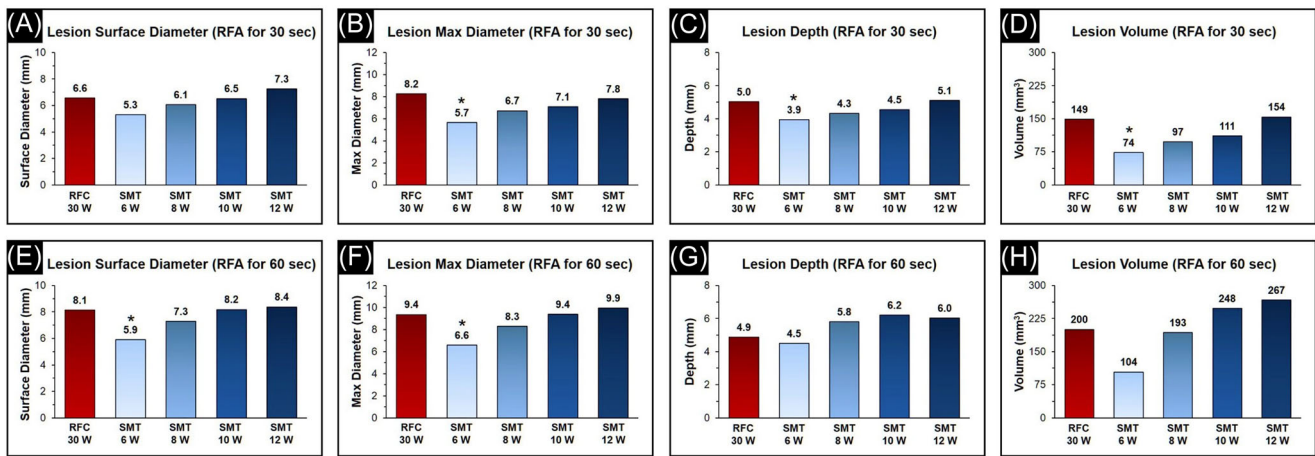


FIGURE 5 RF lesions created using RFC and SMT. Gross and cross-sectional analysis of RF lesions created with RFC (ThermoCool) at 30 W, 30 ml/min, for 30 s (A, C) and SMT at 10 W, 2 ml/min, for 30 s (B, D), respectively. Close-up images of lesions created using RFC (E) and SMT (F), respectively. Lesions generated with SMT were in general more uniform and homogenous with narrower zones of transition. RF, radiofrequency; RFC, radiofrequency ablation catheters



* Significant P-value

FIGURE 6 RF lesion sizes created using RFC and SMT in vivo over porcine thigh muscle preparations. Lesion dimensions including surface diameter, maximum (max) diameter, depth, and volume using RFC (ThermoCool) at 30 W and SMT using varying power (6, 8, 10, and 12 W) for 30 s (A–D) and 60 s (E–H), respectively. RF, radiofrequency; RFC, radiofrequency ablation catheters

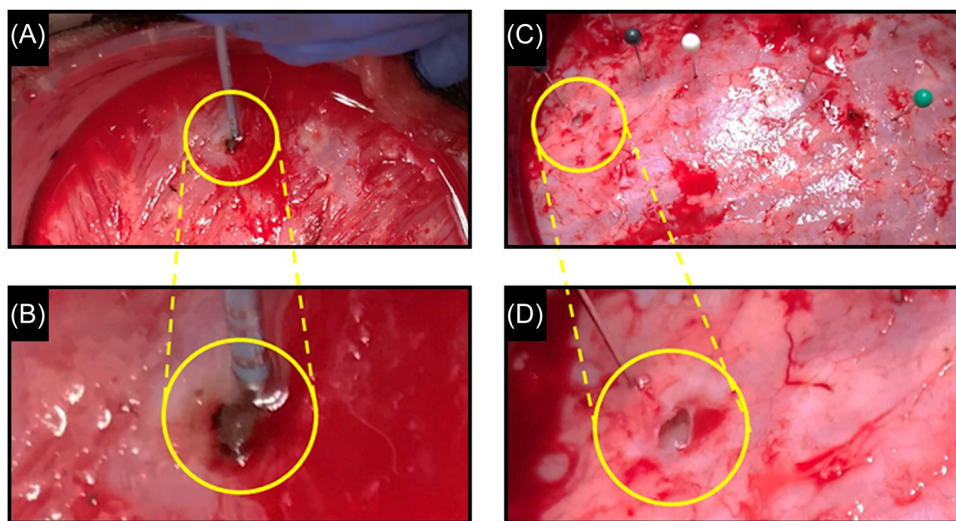


FIGURE 7 Charring and tissue cavitation during in vivo ablation using RFC. Charring (A) and a close-up of the same (B) observed during ablation with RFC (30 W, 30 ml/min, for 30 s). Tissue cavitation in conjunction with a steam pop (C) and a close-up of the same (D) that occurred during ablation using RFC (30 W, 30 ml/min, for 60 s). RFC, radiofrequency ablation catheters

4 | DISCUSSION

During endocardial RFA, the ablation electrode typically in part is in contact with myocardium and in part with the blood pool. However, the impedance of blood is significantly lower than that of myocardial tissue by approximately a factor of two.³ Therefore, the blood pool serves as the preferred route for RF current as it is a significantly better conductor than the targeted myocardium.³ In other instances, the contact/interface between the ablation electrode and blood may even be better than the targeted tissue, further enhancing the flow of RF current into the bloodstream. Meanwhile, upon leaving the electrode–blood–tissue interface, the RF current flows through the patient's chest toward the indifferent electrode. As such, energy is

also in part lost within the nontargeted tissues, including the areas near the skin patches.⁶ The loss of energy within the patient's tissues may vary and depends on the relationship between the impedances of both the patient and the electrode interface.⁷ Prior investigations have estimated that ~38% of the total power delivered during RFA using a standard 4-mm tip catheter is “lost” within the patient (i.e., not utilized in creating a lesion in the targeted tissue), whereas only ~62% of the applied RF energy is delivered “near” the ablation electrode.³ Moreover, when considering a 4-mm ablation electrode, its rounded tip accounts for 25% of the total electrode surface area.³ In the case of a completely perpendicular catheter–tissue alignment, an assumption of 25% electrode–tissue contact may be reasonable. However, this is not always the case with other (nonperfectly perpendicular)

TABLE 3 Ex vivo and in vivo RFA parameters for applications resulting in a steam pop

Power (W)	Irrigation flow rate (ml/min)	Duration (s)	Baseline impedance (Ω)	Minimum/maximum impedance (Ω)	Drop in impedance (%)
SMT					
10	2	30	204	135/172	34
10	2	60	175	129/175	26
10	2	60	188	125/178	34
12	2	30	160	125/164	22
12	2	30	175	135/180	23
12	2	60	199	125/183	37
12	2	60	216	131/150	39
12	2	60	180	118/180	34
RFC					
Ex vivo					
30	30	30	105	80/144	24
30	30	30	98	74/98	24
30	30	60	109	78/143	28
30	30	60	103	80/103	22
30	30	60	87	66/87	24
30	30	60	96	78/86	19
30	30	60	97	86/97	11
30	30	60	98	76/98	22
30	30	60	102	80/86	22
30	30	60	97	77/97	21
30	30	60	105	90/124	14
30	30	60	99	79/99	20
In vivo					
30	30	60	135	125/135	7
30	30	60	110	99/110	10

Abbreviations: RFA, radiofrequency ablation; RFC, radiofrequency ablation catheter.

catheter orientations which can further alter the magnitude of tissue contact. Nonetheless, with the assumption of three-quarter electrode surface contact with blood and only one-quarter electrode surface contact with myocardium, the magnitude of power diverted into the bloodstream during RFA will be roughly six times higher than that which is actually delivered into the tissue.³ When further assuming a 25% tissue contact and ~38% power loss within the patient, the remaining ~62% of the delivered power is split between blood and the tissue in a ratio of 6:1.³ Hence, this implies that only ~9% of the total energy (power) delivered during RFA will typically be applied to the targeted tissue, whereas ~90% of the energy dissipates either into the bloodstream or the nontargeted tissue. Our computational model simulation results were consistent with these prior estimates, predicting that under conditions of the simulation only 13.7% of the RF energy applied using an RFC is directed into the targeted tissue.

It is this concept that led to the development of the SMT catheter. Based on its novel, insulated-tip design, our computational model predicted that the SMT catheter allows for delivery of ~67% of the RF energy into the targeted tissue, in turn, requiring significantly lower power and irrigation to create lesions. This was validated by the evidence from the ex vivo and in vivo studies which found that low power–low irrigation RFA with SMT was indeed capable of creating similar-sized lesions as RFC while utilizing only a fraction of the energy (8–12 vs. 30 W) and irrigation (2 vs. 30 ml/min). Additionally, the computational model predicted a sudden increase in impedance for SMT lesions created at powers above 12 W. Consistent with this, we encountered two steam pops during RFA with SMT at high power (15 W), despite a high irrigation rate (20 ml/min), highlighting the threshold for endocardial convective cooling. Nonetheless, high power–high irrigation (15 W, 20 ml/min)

RFA using SMT proved capable of creating lesions larger and deeper than those generated with RFC which may have clinical implications.

Although RFA using SMT consistently resulted in greater impedance drops, lesions created with SMT at 8–12 W were much less likely to be associated with steam pops, tissue cavitation, or charring as compared to RFC. This is likely attributed to the unique design of the SMT catheter, its electrode tip, more efficient heat transfer characteristics and reduced energy requirements. Specifically, in the “landing gear” configuration, the wings of the SMT catheter stabilize the ablation electrode, preventing it from deeply compressing into the tissue. Consequently, this minimizes ineffective electrode tip cooling, in turn likely resulting in a lower frequency of steam pops as compared with RFC. On the other hand, when ablating with the RFC catheter, the magnitude of force exerted at the electrode tip can significantly impact tissue engagement/contact altering the ratio of current delivery to the tissue versus blood. Since typically with RFC, only a small fraction of the current enters the tissue, modest alterations in this ratio can lead to marked variations in current delivered to the tissue resulting at times in excessive tissue heating and steam pops.

It is also conceivable that ablation using SMT may improve ablation safety by minimizing the risk of collateral injury (e.g., the esophagus) through reduced power and better directing of the RF energy into the targeted tissue. Additionally, a reduction in irrigation coupled with a surface mount thermocouple can result in a more accurate measurement of the tissue temperature by the RFA catheter which too has the potential to improve RFA safety and efficacy in a temperature-controlled mode. Contrary to this, the measured temperature using RFC utilizing relatively-high irrigation rates (i.e., >10 ml/min), is more representative of the temperature of the irrigation fluid as opposed to the myocardial tissue. Lastly, there were significant differences in lesion homogeneity with SMT versus RFC. When ablating with RFC, the electrode–tissue interface is normally sensitive to the forces exerted onto the electrode tip, such that variations may result in nonhomogenous delivery of energy into the targeted tissue, thereby impacting lesion size and morphology. In contrast, owing to its deployable wings (the so-called “landing gear”), SMT is capable of providing a more stable and consistent tissue–electrode contact and interface. Accordingly, in this study, lesions generated using SMT were more homogeneous and exhibited sharper transition zones than those created with RFC. It is conceivable that nonhomogeneity in RFA lesions may account for discrepancies in acute versus long-term lesion efficacy and durability. Hence, it is plausible that the improvements observed in lesion homogeneity could help augment the long-term effectiveness of RFA using this catheter.

4.1 | Limitations

The authors recognize several important limitations in this study. First, the ex vivo and in vivo ablation models do not precisely represent RFA in a clinical scenario. Second, although the tissue was

suspended and the circulation flow was adjusted to simulate the contracting myocardium, the ablated porcine tissue used in both models did not perfectly mimic in vivo cardiac ablation inside a beating heart. Third, in this study, all RFA lesions were created with ablation catheters deployed in a perpendicular orientation to the tissue. Therefore, no conclusions may be reached regarding their performances if positioned in a parallel orientation. Lastly, since the control experiments were only conducted using the ThermoCool RFA catheter, no conclusions may be reached regarding performances or comparisons against other RFA catheters.

5 | CONCLUSIONS

RFA at reduced power (8–12 W) using the novel, insulated-tip SMT ablation catheter is capable of creating lesions comparable in size to those with RFC at 30 W, but with significantly greater impedance drops, yet lower incidences of steam pop, charring, and tissue cavitation, while requiring only 2 ml/min of irrigation rate. On the other hand, high power–high irrigation (15 W, 20 ml/min) RFA using SMT can yield lesions that are significantly larger and deeper than with RFC. Furthermore, lesions generated using SMT are more homogenous with sharper transition zones than those created with RFC.

ACKNOWLEDGMENTS

This study was funded by Sirona Medical Technologies, Inc., the Spanish Ministerio de Ciencia, Innovación y Universidades/Agencia Estatal de Investigación (MCIN/AEI/10.13039/501100011033) (Grant No. RTI2018-094357-B-C21) and the Proyecto UNAJ Investiga 2017 (Grant No. 80020170100019UJ).

DATA AVAILABILITY STATEMENT

Research data are not shared.

ORCID

Arash Aryana  <http://orcid.org/0000-0003-0932-8400>

Enrique Berjano  <http://orcid.org/0000-0002-3247-2665>

Vivek Y. Reddy  <http://orcid.org/0000-0002-5638-4993>

REFERENCES

1. Calkins H, Kuck KH, Cappato R, et al. 2012 HRS/EHRA/ECAS expert consensus statement on catheter and surgical ablation of atrial fibrillation: recommendations for patient selection, procedural techniques, patient management and follow-up, definitions, end-points, and research trial design. *J Interv Card Electrophysiol*. 2011; 33:171-257.
2. Nath S, DiMarco JP, Haines DE. Basic aspects of radiofrequency catheter ablation. *J Cardiovasc Electrophysiol*. 1994;5:863-876.
3. Wittkampf FH, Nakagawa H. RF catheter ablation: lessons on lesions. *Pacing Clin Electrophysiol*. 2006;29:1285-1297.
4. Nakagawa H, Yamanashi WS, Pitha JV, et al. Comparison of in vivo tissue temperature profile and lesion geometry for radiofrequency ablation with a saline-irrigated electrode versus temperature control in a canine thigh muscle preparation. *Circulation*. 1995;91:2264-2273.

5. Demazumder D, Mirotznik MS, Schwartzman D. Biophysics of radiofrequency ablation using an irrigated electrode. *J Interv Card Electrophysiol.* 2001;5:377-389.
6. Nath S, DiMarco JP, Gallop RG, McRury ID, Haines DE. Effects of dispersive electrode position and surface area on electrical parameters and temperature during radiofrequency catheter ablation. *Am J Cardiol.* 1996;77:765-767.
7. Nakagawa H, Wittkamp FHM, Yamanashi WS, et al. Inverse relationship between electrode size and lesion size during radiofrequency ablation with active electrode cooling. *Circulation.* 1998; 98:458-465.

How to cite this article: Aryana A, Irastorza RM, Berjano E, et al. Radiofrequency ablation using a novel insulated-tip ablation catheter can create uniform lesions comparable in size to conventional irrigated ablation catheters while using a fraction of the energy and irrigation. *J Cardiovasc Electrophysiol.* 2022;33:1146-1156.
[doi:10.1111/jce.15461](https://doi.org/10.1111/jce.15461)